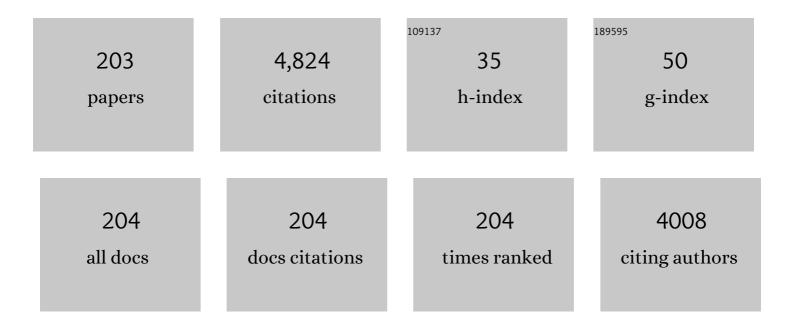
Zhiqiang Zhou

List of Publications by Year in descending order

Source: https://exaly.com/author-pdf/2785755/publications.pdf Version: 2024-02-01



#	Article	IF	CITATIONS
1	Organophosphorus pesticide chlorpyrifos intake promotes obesity and insulin resistance through impacting gut and gut microbiota. Microbiome, 2019, 7, 19.	4.9	149
2	Effects of perinatal exposure to BPA, BPF and BPAF on liver function in male mouse offspring involving in oxidative damage and metabolic disorder. Environmental Pollution, 2019, 247, 935-943.	3.7	89
3	Effects of triphenyl phosphate exposure during fetal development on obesity and metabolic dysfunctions in adult mice: Impaired lipid metabolism and intestinal dysbiosis. Environmental Pollution, 2019, 246, 630-638.	3.7	83
4	The influence of polyethylene microplastics on pesticide residue and degradation in the aquatic environment. Journal of Hazardous Materials, 2020, 394, 122517.	6.5	83
5	In utero and lactational exposure to BDE-47 promotes obesity development in mouse offspring fed a high-fat diet: impaired lipid metabolism and intestinal dysbiosis. Archives of Toxicology, 2018, 92, 1847-1860.	1.9	78
6	Enantioselective toxic effects and biodegradation of benalaxyl in Scenedesmus obliquus. Chemosphere, 2012, 87, 7-11.	4.2	70
7	Neonatal triphenyl phosphate and its metabolite diphenyl phosphate exposure induce sex- and dose-dependent metabolic disruptions in adult mice. Environmental Pollution, 2018, 237, 10-17.	3.7	70
8	Application of a magnetic graphene nanocomposite for organophosphorus pesticide extraction in environmental water samples. Journal of Chromatography A, 2018, 1535, 9-16.	1.8	69
9	Effects of perinatal exposure to BPA and its alternatives (BPS, BPF and BPAF) on hepatic lipid and glucose homeostasis in female mice adolescent offspring. Chemosphere, 2018, 212, 297-306.	4.2	69
10	Toxicity effects in zebrafish embryos (Danio rerio) induced by prothioconazole. Environmental Pollution, 2019, 255, 113269.	3.7	66
11	Enantioselective degradation of fipronil in Chinese cabbage (Brassica pekinensis). Food Chemistry, 2008, 110, 399-405.	4.2	65
12	Neonicotinoid insecticides exposure cause amino acid metabolism disorders, lipid accumulation and oxidative stress in ICR mice. Chemosphere, 2020, 246, 125661.	4.2	65
13	Multifunctional β-Cyclodextrin MOF-Derived Porous Carbon as Efficient Herbicides Adsorbent and Potassium Fertilizer. ACS Sustainable Chemistry and Engineering, 2019, 7, 14479-14489.	3.2	64
14	Joint effects of microplastic and dufulin on bioaccumulation, oxidative stress and metabolic profile of the earthworm (Eisenia fetida). Chemosphere, 2021, 263, 128171.	4.2	61
15	Nonoccupational Exposure to Pyrethroids and Risk of Coronary Heart Disease in the Chinese Population. Environmental Science & Technology, 2017, 51, 664-670.	4.6	60
16	The potential endocrine disruption of pesticide transformation products (TPs): The blind spot of pesticide risk assessment. Environment International, 2020, 137, 105490.	4.8	59
17	A novel magnetic ionic liquid modified carbon nanotube for the simultaneous determination of aryloxyphenoxy-propionate herbicides and their metabolites in water. Analytica Chimica Acta, 2014, 852, 88-96.	2.6	58

18

Enantioselective bioaccumulation of hexaconazole and its toxic effects in adult zebrafish (Danio) Tj ETQq0 0 0 rgBT $_{4.2}^{1/0}$ verlock 10 Tf 50 6

#	Article	IF	CITATIONS
19	The effects of hexaconazole and epoxiconazole enantiomers on metabolic profile following exposure to zebrafish (Danio rerio) as well as the histopathological changes. Chemosphere, 2019, 226, 520-533.	4.2	54
20	Enantioselective Toxic Effects of Hexaconazole Enantiomers Against <i>Scenedesmus Obliquus</i> . Chirality, 2012, 24, 610-614.	1.3	51
21	A simplified procedure for the determination of organochlorine pesticides and polychlorobiphenyls in edible vegetable oils. Food Chemistry, 2014, 151, 47-52.	4.2	50
22	Perinatal exposure to Bisphenol S (BPS) promotes obesity development by interfering with lipid and glucose metabolism in male mouse offspring. Environmental Research, 2019, 173, 189-198.	3.7	50
23	Enantioselective Degradation and Chiral Stability of Malathion in Environmental Samples. Journal of Agricultural and Food Chemistry, 2012, 60, 372-379.	2.4	47
24	1H NMR-based metabolomics analysis of adult zebrafish (Danio rerio) after exposure to diniconazole as well as its bioaccumulation behavior. Chemosphere, 2017, 168, 1571-1577.	4.2	47
25	Enantioselective behavior of malathion enantiomers in toxicity to beneficial organisms and their dissipation in vegetables and crops. Journal of Hazardous Materials, 2012, 237-238, 140-146.	6.5	45
26	Hydrophilic–lipophilic balanced magnetic nanoparticles: Preparation and application in magnetic solid-phase extraction of organochlorine pesticides and triazine herbicides in environmental water samples. Talanta, 2014, 127, 1-8.	2.9	44
27	Effervescence assisted on-site liquid phase microextraction for the determination of five triazine herbicides in water. Journal of Chromatography A, 2014, 1371, 58-64.	1.8	44
28	EnantioselectiveToxic Effects and Degradation of Myclobutanil Enantiomers in <i>Scenedesmus obliquus</i> . Chirality, 2013, 25, 858-864.	1.3	43
29	Antibiotics may increase triazine herbicide exposure risk via disturbing gut microbiota. Microbiome, 2018, 6, 224.	4.9	43
30	Enantioselective bioaccumulation following exposure of adult zebrafish (Danio rerio) to epoxiconazole and its effects on metabolomic profile as well as genes expression. Environmental Pollution, 2017, 229, 264-271.	3.7	42
31	Gut Microbiota: A Key Factor in the Host Health Effects Induced by Pesticide Exposure?. Journal of Agricultural and Food Chemistry, 2020, 68, 10517-10531.	2.4	42
32	Enantiomeric separation of chiral pesticides by high performance liquid chromatography on cellulose tris-3,5-dimethyl carbamate stationary phase under reversed phase conditions. Journal of Separation Science, 2007, 30, 310-321.	1.3	38
33	Distribution, Metabolism and Toxic Effects of Beta-Cypermethrin in Lizards (Eremias argus) Following Oral Administration. Journal of Hazardous Materials, 2016, 306, 87-94.	6.5	38
34	Impacts of Penconazole and Its Enantiomers Exposure on Gut Microbiota and Metabolic Profiles in Mice. Journal of Agricultural and Food Chemistry, 2019, 67, 8303-8311.	2.4	38
35	Enantioselective toxic effects of cyproconazole enantiomers against Chlorella pyrenoidosa. Chemosphere, 2016, 159, 50-57.	4.2	37
36	Bioaccumulation and Metabolism of Carbosulfan in Zebrafish (<i>Danio rerio</i>) and the Toxic Effects of Its Metabolites. Journal of Agricultural and Food Chemistry, 2019, 67, 12348-12356.	2.4	36

#	Article	IF	CITATIONS
37	Ultrafast Removal of Cadmium(II) by Green Cyclodextrin Metal–Organicâ€Frameworkâ€Based Nanoporous Carbon: Adsorption Mechanism and Application. Chemistry - an Asian Journal, 2019, 14, 261-268.	1.7	36
38	Enantioselective toxicity of lactofen and its metabolites in Scenedesmus obliquus. Algal Research, 2015, 10, 72-79.	2.4	35
39	Enantioselective degradation and chiral stability of the herbicide fluazifop-butyl in soil and water. Chemosphere, 2016, 146, 315-322.	4.2	35
40	Pectin reduces environmental pollutant-induced obesity in mice through regulating gut microbiota: A case study of p,p′-DDE. Environment International, 2019, 130, 104861.	4.8	35
41	Developmental toxicity and neurotoxicity of penconazole enantiomers exposure on zebrafish (Danio) Tj ETQq1	1 0.784314 3.7	4 rggT /Oved
42	New insights into bisphenols induced obesity in zebrafish (Danio rerio): Activation of cannabinoid receptor CB1. Journal of Hazardous Materials, 2021, 418, 126100.	6.5	35
43	Stereoselective toxicity of metconazole to the antioxidant defenses and the photosynthesis system of Chlorella pyrenoidosa. Aquatic Toxicology, 2019, 210, 129-138.	1.9	34
44	Enantioselective toxic effects and environmental behavior of ethiprole and its metabolites against Chlorella pyrenoidosa. Environmental Pollution, 2019, 244, 757-765.	3.7	33
45	Effects of exposure to prothioconazole and its metabolite prothioconazole-desthio on oxidative stress and metabolic profiles of liver and kidney tissues in male mice. Environmental Pollution, 2021, 269, 116215.	3.7	33
46	Effects of antibiotic norfloxacin on the degradation and enantioselectivity of the herbicides in aquatic environment. Ecotoxicology and Environmental Safety, 2021, 208, 111717.	2.9	32
47	Stereoselective metabolism of fipronil in water hyacinth (Eichhornia crassipes). Pesticide Biochemistry and Physiology, 2010, 97, 289-293.	1.6	31
48	Chiral Insecticide α-Cypermethrin and Its Metabolites: Stereoselective Degradation Behavior in Soils and the Toxicity to Earthworm <i>Eisenia fetida</i> . Journal of Agricultural and Food Chemistry, 2015, 63, 7714-7720.	2.4	31
49	Effervescence assisted dispersive liquid-liquid microextraction based on cohesive floating organic drop for the determination of herbicides and fungicides in water and grape juice. Food Chemistry, 2018, 245, 653-658.	4.2	31
50	Determination of Organophosphorus Pesticides in Soybean Oil, Peanut Oil and Sesame Oil by Low-Temperature Extraction and GC-FPD. Chromatographia, 2007, 66, 625-629.	0.7	30
51	A simple method for the determination of organochlorine pollutants and the enantiomers in oil seeds based on matrix solid-phase dispersion. Food Chemistry, 2016, 194, 319-324.	4.2	30
52	Toxicity and metabolomics study of isocarbophos in adult zebrafish (Danio rerio). Ecotoxicology and Environmental Safety, 2018, 163, 1-6.	2.9	30
53	Different Toxic Effects of Racemate, Enantiomers, and Metabolite of Malathion on HepG2 Cells Using High-Performance Liquid Chromatography–Quadrupole–Time-of-Flight-Based Metabolomics. Journal of Agricultural and Food Chemistry, 2019, 67, 1784-1794.	2.4	30
54	Different effects of exposure to penconazole and its enantiomers on hepatic glycolipid metabolism of male mice. Environmental Pollution, 2020, 257, 113555.	3.7	30

#	Article	IF	CITATIONS
55	A full evaluation of chiral phenylpyrazole pesticide flufiprole and the metabolites to non-target organism in paddy field. Environmental Pollution, 2020, 264, 114808.	3.7	30
56	Enantioselective phytotoxicity and bioacitivity of the enantiomers of the herbicide napropamide. Pesticide Biochemistry and Physiology, 2015, 125, 38-44.	1.6	29
57	Fipronil-induced enantioselective developmental toxicity to zebrafish embryo-larvae involves changes in DNA methylation. Scientific Reports, 2017, 7, 2284.	1.6	29
58	New insight into the mechanism of POP-induced obesity: Evidence from DDE-altered microbiota. Chemosphere, 2020, 244, 125123.	4.2	29
59	Approach for Pesticide Residue Analysis for Metabolite Prothioconazole-desthio in Animal Origin Food. Journal of Agricultural and Food Chemistry, 2017, 65, 2481-2487.	2.4	28
60	A combined NMR- and HPLC-MS/MS-based metabolomics to evaluate the metabolic perturbations and subacute toxic effects of endosulfan on mice. Environmental Science and Pollution Research, 2017, 24, 18870-18880.	2.7	28
61	The enantioselective environmental behavior and toxicological effects of pyriproxyfen in soil. Journal of Hazardous Materials, 2019, 365, 97-106.	6.5	28
62	Perinatal exposure to 2-Ethylhexyl Diphenyl Phosphate (EHDPHP) affected the metabolic homeostasis of male mouse offspring: Unexpected findings help to explain dose- and diet- specific phenomena. Journal of Hazardous Materials, 2020, 388, 122034.	6.5	28
63	Singleâ€Drop Microextraction and Gas Chromatographic Determination of Fungicide in Water and Wine Samples. Analytical Letters, 2006, 39, 2333-2344.	1.0	27
64	Bioaccumulation of isocarbophos enantiomers from laboratory-contaminated aquatic environment by tubificid worms. Chemosphere, 2015, 124, 77-82.	4.2	27
65	Enantioselective accumulation, metabolism and phytoremediation of lactofen by aquatic macrophyte Lemna minor. Ecotoxicology and Environmental Safety, 2017, 143, 186-192.	2.9	27
66	Perinatal exposure to low-dose decabromodiphenyl ethane increased the risk of obesity in male mice offspring. Environmental Pollution, 2018, 243, 553-562.	3.7	27
67	The effect of biochar on the mitigation of the chiral insecticide fipronil and its metabolites burden on loach (Misgurnus.anguillicaudatus). Journal of Hazardous Materials, 2018, 360, 214-222.	6.5	27
68	Magnetic partially carbonized cellulose nanocrystal-based magnetic solid phase extraction for the analysis of triazine and triazole pesticides in water. Mikrochimica Acta, 2019, 186, 825.	2.5	27
69	Direct enantiomeric separation of chiral pesticides by liquid chromatography on polysaccharide-based chiral stationary phases under reversed phase conditions. Analytical Methods, 2012, 4, 2307.	1.3	26
70	A full evaluation for the enantiomeric impacts of lactofen and its metabolites on aquatic macrophyte Lemna minor. Water Research, 2016, 101, 55-63.	5.3	26
71	Chiral quizalofop-ethyl and its metabolite quizalofop-acid in soils: Enantioselective degradation, enzymes interaction and toxicity to Eisenia foetida. Chemosphere, 2016, 152, 173-180.	4.2	25
72	Combined ingestion of polystyrene microplastics and epoxiconazole increases health risk to mice: Based on their synergistic bioaccumulation in vivo. Environment International, 2022, 166, 107391.	4.8	25

#	Article	IF	CITATIONS
73	Stereoselective pharmacokinetics of diniconazole enantiomers in rabbits. Chirality, 2009, 21, 699-703.	1.3	24
74	The effect of antibiotics on the persistence of herbicides in soil under the combined pollution. Chemosphere, 2018, 204, 303-309.	4.2	24
75	Enantioselective mechanism of toxic effects of triticonazole against Chlorella pyrenoidosa. Ecotoxicology and Environmental Safety, 2019, 185, 109691.	2.9	24
76	The biological activities of prothioconazole enantiomers and their toxicity assessment on aquatic organisms. Chirality, 2019, 31, 468-475.	1.3	24
77	Amphibian (Rana nigromaculata)exposed to cyproconazole: Changes in growth index, behavioral endpoints, antioxidant biomarkers, thyroid and gonad development. Aquatic Toxicology, 2019, 208, 62-70.	1.9	24
78	Exposure to nitenpyram during pregnancy causes colonic mucosal damage and non-alcoholic steatohepatitis in mouse offspring: The role of gut microbiota. Environmental Pollution, 2021, 271, 116306.	3.7	24
79	Systematic evaluation of chiral pesticides at the enantiomeric level: A new strategy for the development of highly effective and less harmful pesticides. Science of the Total Environment, 2022, 846, 157294.	3.9	24
80	Enantioselective Bioaccumulation, Tissue Distribution, and Toxic Effects of Myclobutanil Enantiomers in <i>Pelophylax nigromaculatus</i> Tadpole. Journal of Agricultural and Food Chemistry, 2017, 65, 3096-3102.	2.4	23
81	Comparison of triadimefon and its metabolite on acute toxicity and chronic effects during the early development of Rana nigromaculata tadpoles. Ecotoxicology and Environmental Safety, 2018, 156, 247-254.	2.9	23
82	Impaired lipid and glucose homeostasis in male mice offspring after combined exposure to low-dose bisphenol A and arsenic during the second half of gestation. Chemosphere, 2018, 210, 998-1005.	4.2	23
83	Stereoselective quantitation of haloxyfop in environment samples and enantioselective degradation in soils. Chemosphere, 2015, 119, 583-589.	4.2	22
84	Imbalance of gut microbiota and fecal metabolites in offspring female mice induced by nitenpyram exposure during pregnancy. Chemosphere, 2020, 260, 127506.	4.2	22
85	HPLC Separation of Metalaxyl and Metalaxyl Intermediate Enantiomers on Celluloseâ€Based Sorbent. Analytical Letters, 2004, 37, 167-173.	1.0	21
86	Enantioselective degradation of the chiral alpha-cypermethrin and detection of its metabolites in five plants. Environmental Science and Pollution Research, 2019, 26, 1558-1564.	2.7	21
87	Toxicity risk assessment of pyriproxyfen and metabolites in the rat liver: A vitro study. Journal of Hazardous Materials, 2020, 389, 121835.	6.5	21
88	Assessment of toxicity and environmental behavior of chiral ethiprole and its metabolites using zebrafish model. Journal of Hazardous Materials, 2021, 414, 125492.	6.5	21
89	Evaluating the effects of the tebuconazole on the earthworm, Eisenia fetida by H-1 NMR-Based untargeted metabolomics and mRNA assay. Ecotoxicology and Environmental Safety, 2020, 194, 110370.	2.9	19
90	Fate and Stereoselective Behavior of Benalaxyl in a Water–Sediment Microcosm. Journal of Agricultural and Food Chemistry, 2015, 63, 5205-5211.	2.4	18

#	Article	IF	CITATIONS
91	Effects of wastewater irrigation and sewage sludge application on soil residues of chiral fungicide benalaxyl. Environmental Pollution, 2017, 224, 1-6.	3.7	18
92	Assessment of tissue-specific accumulation, elimination and toxic effects of dichlorodiphenyltrichloroethanes (DDTs) in carp through aquatic food web. Scientific Reports, 2017, 7, 2288.	1.6	18
93	Exposure of frogs and tadpoles to chiral herbicide fenoxaprop-ethyl. Chemosphere, 2017, 186, 832-838.	4.2	18
94	Enantioselective toxic effects of cyproconazole enantiomers against Rana nigromaculata. Environmental Pollution, 2018, 243, 1825-1832.	3.7	18
95	1H NMR-based serum metabolomics analysis of the age-related metabolic effects of perinatal exposure to BPA, BPS, BPF, and BPAF in female mice offspring. Environmental Science and Pollution Research, 2019, 26, 5804-5813.	2.7	18
96	Effects of incremental endosulfan sulfate exposure and high fat diet on lipid metabolism, glucose homeostasis and gut microbiota in mice. Environmental Pollution, 2021, 268, 115697.	3.7	18
97	Multi-Encapsulation Combination of O/W/O Emulsions with Polyurea Microcapsules for Controlled Release and Safe Application of Dimethyl Disulfide. ACS Applied Materials & Interfaces, 2021, 13, 1333-1344.	4.0	18
98	Accumulation, distribution and removal of triazine pesticides by Eichhornia crassipes in water-sediment microcosm. Ecotoxicology and Environmental Safety, 2021, 219, 112236.	2.9	18
99	Simultaneous determination of paclobutrazol and myclobutanil enantiomers in water and soil using enantioselective reversed-phase liquid chromatography. Analytical Methods, 2010, 2, 617.	1.3	17
100	Monitoring tryptophan metabolism after exposure to hexaconazole and the enantioselective metabolism of hexaconazole in rat hepatocytes in vitro. Journal of Hazardous Materials, 2015, 295, 9-16.	6.5	17
101	Enantioselective bioaccumulation and metabolism of lactofen in zebrafish Danio rerio and combined effects with its metabolites. Chemosphere, 2018, 213, 443-452.	4.2	17
102	Toxicity and fate of chiral insecticide pyriproxyfen and its metabolites in zebrafish (Danio rerio). Environmental Pollution, 2021, 280, 116894.	3.7	17
103	Direct Enantiomeric Separation of Chiral Pesticides by LC on Amylose Tris(3,5-dimethylphenylcarbamate) Stationary Phase under Reversed Phase Conditions. Chromatographia, 2010, 71, 855-865.	0.7	16
104	Environmental Fate of Chiral Herbicide Fenoxaprop-ethyl in Water-Sediment Microcosms. Scientific Reports, 2016, 6, 26797.	1.6	16
105	Enantioselective toxicity and bioaccumulation of epoxiconazole enantiomers to the green alga Scenedesmus obliquus. RSC Advances, 2016, 6, 59842-59850.	1.7	16
106	NMR- and LC–MS/MS-based urine metabolomic investigation of the subacute effects of hexabromocyclododecane in mice. Environmental Science and Pollution Research, 2016, 23, 8500-8507.	2.7	16
107	Direct chiral separations of the enantiomers of phenylpyrazole pesticides and the metabolites by HPLC. Chirality, 2017, 29, 19-25.	1.3	16
108	Effects of the Chiral Fungicides Metalaxyl and Metalaxyl-M on the Earthworm Eisenia fetida as Determined by 1H-NMR-Based Untargeted Metabolomics. Molecules, 2019, 24, 1293.	1.7	16

Zhiqiang Zhou

#	Article	IF	CITATIONS
109	Tissue Distribution, Accumulation, and Metabolism of Chiral Flufiprole in Loach (<i>Misgurnus) Tj ETQq1 1 0.7843</i>	14 rgBT /C 2.4	Dyerlock 10
110	Occurrence and migration of phthalates in adhesive materials to fruits and vegetables. Journal of Hazardous Materials, 2021, 418, 126277.	6.5	16
111	Enantioselective Fungicidal Activity and Toxicity to Early Wheat Growth of the Chiral Pesticide Triticonazole. Journal of Agricultural and Food Chemistry, 2021, 69, 11154-11162.	2.4	16
112	Enantioselective degradation of prothioconazole in soil and the impacts on the enzymes and microbial community. Science of the Total Environment, 2022, 824, 153658.	3.9	16
113	Evaluating the enantioselective degradation and novel metabolites following a single oral dose of metalaxyl in mice. Pesticide Biochemistry and Physiology, 2014, 116, 32-39.	1.6	15
114	Enantioselective dissipation of pyriproxyfen in soils and sand. Chirality, 2017, 29, 358-368.	1.3	15
115	The influence of oxytetracycline on the degradation and enantioselectivity of the chiral pesticide beta-cypermethrin in soil. Environmental Pollution, 2019, 255, 113215.	3.7	15
116	Distribution, metabolism and metabolic disturbances of alpha-cypermethrin in embryo development, chick growth and adult hens. Environmental Pollution, 2019, 249, 390-397.	3.7	15
117	Effect of triadimefon and its metabolite on adult amphibians Xenopus laevis. Chemosphere, 2020, 243, 125288.	4.2	15
118	Prothioconazole and prothioconazole-desthio induced different hepatotoxicities via interfering with glycolipid metabolism in mice. Pesticide Biochemistry and Physiology, 2022, 180, 104983.	1.6	15
119	pH-controlled quaternary ammonium herbicides capture/release by carboxymethyl-β-cyclodextrin functionalized magnetic adsorbents: Mechanisms and application. Analytica Chimica Acta, 2015, 901, 51-58.	2.6	14
120	Enantiomeric Separation of Chiral Pesticides by Permethylated β yclodextrin Stationary Phase in Reversed PhaseLiquid Chromatography. Chirality, 2016, 28, 409-414.	1.3	14
121	Comparison of subacute effects of two types of pyrethroid insecticides using metabolomics methods. Pesticide Biochemistry and Physiology, 2017, 143, 161-167.	1.6	14
122	Bioaccumulation, behavior changes and physiological disruptions with gender-dependent in lizards (Eremias argus) after exposure to glufosinate-ammonium and l-glufosinate-ammonium. Chemosphere, 2019, 226, 817-824.	4.2	14
123	Different effects of α-endosulfan, β-endosulfan, and endosulfan sulfate on sex hormone levels, metabolic profile and oxidative stress in adult mice testes. Environmental Research, 2019, 169, 315-325.	3.7	14
124	Hepatotoxicity and reproductive disruption in male lizards (Eremias argus) exposed to glufosinate-ammonium contaminated soil. Environmental Pollution, 2019, 246, 190-197.	3.7	14
125	Catechol Dyes–Tyrosinase System for Colorimetric Determination and Discrimination of Dithiocarbamate Pesticides. Journal of Agricultural and Food Chemistry, 2020, 68, 9252-9259.	2.4	14
126	Enantiomeric separation of malathion and malaoxon and the chiral residue analysis in food and environmental matrix. Chirality, 2020, 32, 1053-1061.	1.3	14

#	Article	IF	CITATIONS
127	Perfluorooctanoic acid exposure impact a trade-off between self-maintenance and reproduction in lizards (Eremias argus) in a gender-dependent manner. Environmental Pollution, 2020, 262, 114341.	3.7	14
128	Biodegradation of Chiral Flufiprole in <i>Chlorella pyrenoidosa</i> : Kinetics, Transformation Products, and Toxicity Evaluation. Journal of Agricultural and Food Chemistry, 2020, 68, 1966-1973.	2.4	14
129	Application of liquid-phase microextraction and gas chromatography to the determination of chlorfenapyr in water samples. Mikrochimica Acta, 2008, 162, 161-165.	2.5	13
130	Stereoselective metabolism of benalaxyl in liver microsomes from rat and rabbit. Chirality, 2011, 23, 93-98.	1.3	13
131	Enantioselective metabolism of the chiral herbicide diclofop-methyl and diclofop by HPLC in loach (Misgurnus anguillicaudatus) liver microsomes in vitro. Journal of Chromatography B: Analytical Technologies in the Biomedical and Life Sciences, 2014, 969, 132-138.	1.2	13
132	A combined non-targeted and targeted metabolomics approach to study the stereoselective metabolism of benalaxyl enantiomers in mouse hepatic microsomes. Environmental Pollution, 2016, 212, 358-365.	3.7	13
133	Polymer-coated magnetic nanospheres for preconcentration of organochlorine and pyrethroid pesticides prior to their determination by gas chromatography with electron capture detection. Mikrochimica Acta, 2016, 183, 1187-1194.	2.5	13
134	Metabolomics Approach to Investigate Estrogen Receptor-Dependent and Independent Effects of o,pâ€2-DDT in the Uterus and Brain of Immature Mice. Journal of Agricultural and Food Chemistry, 2017, 65, 3609-3616.	2.4	13
135	Enantioselective metabolism and enantiomerization of benalaxyl in mice. Chemosphere, 2017, 169, 308-315.	4.2	13
136	Gut microbiome alterations induced by tributyltin exposure are associated with increased body weight, impaired glucose and insulin homeostasis and endocrine disruption in mice. Environmental Pollution, 2020, 266, 115276.	3.7	13
137	A common fungicide tebuconazole promotes colitis in mice via regulating gut microbiota. Environmental Pollution, 2022, 292, 118477.	3.7	13
138	A Typical Fungicide and Its Main Metabolite Promote Liver Damage in Mice through Impacting Gut Microbiota and Intestinal Barrier Function. Journal of Agricultural and Food Chemistry, 2021, 69, 13436-13447.	2.4	13
139	Enantioselective Metabolism and Interference on Tryptophan Metabolism of Myclobutanil in Rat Hepatocytes. Chirality, 2015, 27, 643-649.	1.3	12
140	Toxicokinetics and oxidative stress in Tubifex tubifex exposed to hexachlorocyclohexane isomers. RSC Advances, 2016, 6, 19016-19024.	1.7	12
141	The fate of technical-grade chlordane in mice fed a high-fat diet and its roles as a candidate obesogen. Environmental Pollution, 2017, 222, 532-542.	3.7	12
142	Deep eutectic solvent-based liquid phase microextraction for the determination of pharmaceuticals and personal care products in fish oil. New Journal of Chemistry, 2017, 41, 15105-15109.	1.4	12
143	Tissue distribution and toxicity effects of myclobutanil enantiomers in lizards (Eremias argus). Ecotoxicology and Environmental Safety, 2017, 145, 623-629.	2.9	12
144	Supramolecular fluorescent sensor array for simultaneous qualitative and quantitative analysis of quaternary ammonium herbicides. New Journal of Chemistry, 2018, 42, 17317-17322.	1.4	12

#	Article	IF	CITATIONS
145	Stereoselective Physiological Effects of Metconazole on Seed Germination and Seedling Growth of Wheat. Journal of Agricultural and Food Chemistry, 2020, 68, 11672-11683.	2.4	12
146	Bioaccumulation and toxic effects of penconazole in earthworms (Eisenia fetida) following soil exposure. Environmental Science and Pollution Research, 2020, 27, 38056-38063.	2.7	12
147	Effects of simazine and food deprivation chronic stress on energy allocation among the costly physiological processes of male lizards (Eremias argus). Environmental Pollution, 2021, 269, 116139.	3.7	12
148	Systematic investigation of stereochemistry, stereoselective bioactivity, and antifungal mechanism of chiral triazole fungicide metconazole. Science of the Total Environment, 2021, 784, 147194.	3.9	12
149	Risk Assessment of the Chiral Fungicide Triticonazole: Enantioselective Effects, Toxicity, and Fate. Journal of Agricultural and Food Chemistry, 2022, 70, 2712-2721.	2.4	12
150	Enantioselective Characteristics and Montmorillonite-Mediated Removal Effects of α-Hexachlorocyclohexane in Laying Hens. Environmental Science & Technology, 2016, 50, 5695-5701.	4.6	11
151	Discrepant effects of α-endosulfan, β-endosulfan, and endosulfan sulfate on oxidative stress and energy metabolism in the livers and kidneys of mice. Chemosphere, 2018, 205, 223-233.	4.2	11
152	Fluorometric atrazine assay based on the use of nitrogen-doped graphene quantum dots and on inhibition of the activity of tyrosinase. Mikrochimica Acta, 2019, 186, 527.	2.5	11
153	Enantioselective behaviour of the herbicide fluazifop-butyl in vegetables and soil. Food Chemistry, 2017, 221, 1120-1127.	4.2	10
154	Chiral pyrethroid insecticide fenpropathrin and its metabolite: enantiomeric separation and pharmacokinetic degradation in soils by reverse-phase high-performance liquid chromatography. Analytical Methods, 2017, 9, 4439-4446.	1.3	10
155	Absorption, Distribution, Metabolism, and in Vitro Digestion of Beta-Cypermethrin in Laying Hens. Journal of Agricultural and Food Chemistry, 2017, 65, 7647-7652.	2.4	10
156	Stereoselective metabolism and potential adverse effects of chiral fungicide triadimenol on Eremias argus. Environmental Science and Pollution Research, 2020, 27, 7823-7834.	2.7	10
157	Synergistic effect of ZnO NPs and imidacloprid on liver injury in male ICR mice: Increase the bioavailability of IMI by targeting the gut microbiota. Environmental Pollution, 2022, 294, 118676.	3.7	10
158	Effects of three surfactants on the degradation and environmental risk of metolachlor in aquatic environment. Chemosphere, 2022, 300, 134295.	4.2	10
159	Determination of DNA with Imidacloprid by a Resonance Light Scattering Technique at Nanogram Levels and Its Application. Analytical Letters, 2004, 37, 1339-1354.	1.0	9
160	Direct Optical Resolution of Chiral Pesticides by High Performance Liquid Chromatography on Cellulose trisâ€3,5â€Dimethylphenyl Carbamate Stationary Phase Under Reversed Phase Conditions. Journal of Liquid Chromatography and Related Technologies, 2004, 27, 2935-2944.	0.5	9
161	Direct Optical Resolution of Chiral Pesticides by HPLC on Emamectin CSP under Normal Phase Conditions. Journal of Liquid Chromatography and Related Technologies, 2006, 29, 1601-1607.	0.5	9
162	Food Safety: Monitoring of Organophosphate Pesticide Residues in Crops and Food. Phosphorus, Sulfur and Silicon and the Related Elements, 2008, 183, 280-290.	0.8	9

#	Article	IF	CITATIONS
163	Enantioselective metabolism and toxic effects of metalaxyl on primary hepatocytes from rat. Environmental Science and Pollution Research, 2016, 23, 18649-18656.	2.7	9
164	Selective bioaccumulation and elimination of hexachlorocyclohexane isomers in Tubifex tubifex (Oligochaeta, Tubificidae). Environmental Science and Pollution Research, 2016, 23, 6990-6998.	2.7	9
165	Enantioselective degradation of alpha-cypermethrin and detection of its metabolites in bullfrog () Tj ETQq1 1 0.78	34314 rgB ⁻ 2.9	Г ¦Overloc <mark>k</mark>
166	Determination of cyanamide residue in 21 plant-derived foods by liquid chromatography-tandem mass spectrometry. Food Chemistry, 2018, 239, 529-534.	4.2	9
167	Subacute oral toxicity assessment of benalaxyl in mice based on metabolomics methods. Chemosphere, 2018, 191, 373-380.	4.2	9
168	Ecological risk assessment of alpha-cypermethrin-treated food ingestion and reproductive toxicity in reptiles. Ecotoxicology and Environmental Safety, 2019, 171, 657-664.	2.9	9
169	Thermal effects on tissue distribution, liver biotransformation, metabolism and toxic responses in Mongolia racerunner (Eremias argus) after oral administration of beta-cyfluthrin. Environmental Research, 2020, 185, 109393.	3.7	9
170	The stereoselectivity of metconazole on wheat grain filling and harvested seeds germination: Implication for the application of triazole chiral pesticides. Journal of Hazardous Materials, 2021, 416, 125911.	6.5	9
171	Enantioselective Degradation and Chiral Stability of Metalaxylâ€M in Tomato Fruits. Chirality, 2016, 28, 382-386.	1.3	8
172	Enantiomeric Separations of Pyriproxyfen and its Six Chiral Metabolites by Highâ€₽erformance Liquid Chromatography. Chirality, 2016, 28, 245-252.	1.3	8
173	Matrix Solid-Phase Dispersion Combined with GC–MS/MS for the Determination of Organochlorine Pesticides and Polychlorinated Biphenyls in Marketed Seafood. Chromatographia, 2017, 80, 813-824.	0.7	8
174	Effects of cis-bifenthrin enantiomers on the growth, behavioral, biomarkers of oxidative damage and bioaccumulation in Xenopus laevis. Aquatic Toxicology, 2019, 214, 105237.	1.9	8
175	Effects of beta-cypermethrin and myclobutanil on some enzymes and changes of biomarkers between internal tissues and saliva in reptiles (Eremias argus). Chemosphere, 2019, 216, 69-74.	4.2	8
176	Effects of L-Glufosinate-ammonium and temperature on reproduction controlled by neuroendocrine system in lizard (Eremias argus). Environmental Pollution, 2020, 257, 113564.	3.7	8
177	Biomarkers in Tubifex tubifex for the metalaxyl and metalaxyl-M toxicity assessment in artificial sediment. Environmental Science and Pollution Research, 2017, 24, 3618-3625.	2.7	7
178	Enantioselective dissipation of pyriproxyfen in soil under fertilizers use. Ecotoxicology and Environmental Safety, 2019, 167, 404-411.	2.9	7
179	Comparing alpha-cypermethrin induced dose/gender-dependent responses of lizards in hepatotoxicity and nephrotoxicity in a food chain. Chemosphere, 2020, 256, 127069.	4.2	7
180	Hexaconazole Application Saves the Loss of Grey Mold Disease but Hinders Tomato Fruit Ripening in Healthy Plants. Journal of Agricultural and Food Chemistry, 2022, 70, 3948-3957.	2.4	7

Zhiqiang Zhou

#	Article	IF	CITATIONS
181	Combined effects of abamectin and temperature on the physiology and behavior of male lizards (Eremias argus): Clarifying adaptation and maladaptation. Science of the Total Environment, 2022, 837, 155794.	3.9	7
182	Chiral Separation and Enantioselective Degradation of Vinclozolin in Soils. Chirality, 2014, 26, 155-159.	1.3	6
183	Evaluating the enantioselective distribution, degradation and excretion of epoxiconazole in mice following a single oral gavage. Xenobiotica, 2015, 45, 1009-1015.	0.5	6
184	Stereoselective Degradation of alphaâ€Cypermethrin and Its Enantiomers in Rat Liver Microsomes. Chirality, 2016, 28, 58-64.	1.3	6
185	Effects of benthic organism Tubifex tubifex on hexachlorocyclohexane isomers transfer and distribution into freshwater sediment. Ecotoxicology and Environmental Safety, 2016, 126, 163-169.	2.9	6
186	Selective bioaccumulation, biomagnification, and dissipation of hexachlorocyclohexane isomers in a freshwater food chain. Environmental Science and Pollution Research, 2018, 25, 18752-18761.	2.7	6
187	Combination of modified biochar and polyurea microcapsules to coâ€encapsulate a fumigant via interface polymerization for controlled release and enhanced bioactivity. Pest Management Science, 2022, 78, 73-85.	1.7	6
188	Comparative toxic responses of male and female lizards (Eremias argus) exposed to (S)-metolachlor-contaminated soil. Environmental Pollution, 2017, 227, 476-483.	3.7	5
189	Enantioselectivity effects of imazethapyr enantiomers to metabolic responses in mice. Pesticide Biochemistry and Physiology, 2020, 168, 104619.	1.6	5
190	Effects of penconazole enantiomers exposure on hormonal disruption in zebrafish Danio rerio (Hamilton, 1822). Environmental Science and Pollution Research, 2021, 28, 43476-43482.	2.7	5
191	Effects of Cd2+ and Pb2+ on enantioselective degradation behavior of α-cypermethrin in soils and their combined effect on activities of soil enzymes. Environmental Science and Pollution Research, 2021, 28, 47099-47106.	2.7	5
192	Evaluation of organochlorine pesticides in soil using ultrasound-assisted liquid phase microextraction. Analytical Methods, 2015, 7, 1366-1371.	1.3	4
193	Comparing the effect of triadimefon and its metabolite on male and female Xenopus laevis: Obstructed growth and gonad morphology. Chemosphere, 2020, 259, 127415.	4.2	4
194	Tyrosinase coupled with boron-doped carbon nanodots for fluorometric determination of dithiocarbamate fungicide ziram. Microchemical Journal, 2021, 166, 106241.	2.3	4
195	Enantioselective Metabolism of Quizalofop-Ethyl in Rat. PLoS ONE, 2014, 9, e101052.	1.1	4
196	Enantioselective characteristics, bioaccumulation and toxicological effects of chlordane-related compounds in laying hens. Chemosphere, 2022, 300, 134486.	4.2	4
197	A Simple Method for the Determination of Pharmaceutical and Personal Care Products in Fish Tissue Based on Matrix Solid-Phase Dispersion. Journal of Agricultural and Food Chemistry, 2021, 69, 15738-15745.	2.4	4
198	Minimizing geometric isomerization of α-cypermethrin in the residue analysis. Food Chemistry, 2016, 196, 828-832.	4.2	3

#	Article	IF	CITATIONS
199	Thermoregulation of Eremias argus alters temperature-dependent toxicity of beta-cyfluthrin: Ecotoxicological effects considering ectotherm behavior traits. Environmental Pollution, 2022, 293, 118461.	3.7	3
200	Effects of Dufulin on Oxidative Stress and Metabolomic Profile of Tubifex. Metabolites, 2021, 11, 381.	1.3	2
201	The enantioselective metabolic mechanism of quizalofop-ethyl and quizalofop-acid enantiomers in animal: protein binding, intestinal absorption, and in vitro metabolism in plasma and the microsome. RSC Advances, 2016, 6, 99003-99009.	1.7	1
202	Analysis of volatile organic compounds in environmental matrices by nitrogen-assisted headspace solid-phase extraction. New Journal of Chemistry, 2019, 43, 8788-8795.	1.4	1
203	HEATS OF FORMATION FOR BORON COMPOUNDS BASED ON QUANTUM CHEMICAL CALCULATIONS. Journal of Theoretical and Computational Chemistry, 2010, 09, 1009-1019.	1.8	0